Polymer Testing 112 (2022) 107623

Contents lists available at ScienceDirect

Polymer Testing

journal homepage: www.elsevier.com/locate/polytest

Weathering-induced oxidation: An investigation of artificially aged polystyrene samples using Laser-induced Breakdown Spectroscopy

Caroline Sommer [a,*], Johnny Nguyen [a], Teresa Menzel [b], Julia A. Prume [a,c], Holger Ruckdäschel [b], Martin Koch [a]

[a] Faculty of Physics and Material Sciences Centre, Philipps-University Marburg, 35037 Marburg, Germany
[b] Department Polymer Engineering, University of Bayreuth, 95447 Bayreuth, Germany
[c] Bayreuth Graduate School of Mathematical and Natural Sciences (BayNAT), University of Bayreuth, 95447 Bayreuth, Germany

ARTICLE INFO

Keywords:
Laser-induced Breakdown Spectroscopy
Weathering-induced oxidation
Polystyrene
Plastic degradation
Surface and depth profile analysis

ABSTRACT

This study discusses weathering-induced oxidation of polystyrene with and without different concentrations of the antioxidant Irgafos using Laser-induced Breakdown Spectroscopy (LIBS). By examining the spectral feature of oxidation and due to laser ablation, a systematical analysis of the oxygen content on the sample's surface and its penetration depth could be conducted. The results show that LIBS can be used as a fast technique for the quantification of weathering-induced oxidation.

1. Introduction

Plastic litter is a rapidly emerging health hazard that is in dire need for global action [1–4]. Most prominently, it is associated with waste in our marine environment which accounts for roughly 8 MT of the global plastic litter produced annually [1]. Once released in the open water, they are exposed to harsh conditions, such as sunlight exposure and mechanical stress. Such conditions are in stark contrast to those intended for most consumer plastic products. As a result, their material properties deteriorate with time which promotes fragmentation where a material breaks up into smaller pieces. Particles with sizes less than 5 mm, commonly termed as secondary microplastics [5], are particularly concerning as they have already been detected in multiple types of organisms including the human body [6–10]. This is precisely why we urgently need assessments of the long-term effects of (secondary micro-) plastics on our ecosystem and mitigation schemes to keep their potential detrimental effect to a minimum. Both, however, require a much better understanding of the interaction between plastics and the environment that could ultimately help make plastics more biodegradable and thus contribute to a reduction in plastic litter.

Plastic degradation in our environment is the result of numerous physical, chemical and biological processes that can occur over time scales of months and years [11]. Studying these processes is not straightforward as they can also vary with the chemical composition of the starting material [12]. Studies on degradation usually analyze the influence of the most essential environmental process on a selection of plastic litter types by recreating them in the lab. By adjusting the environmental parameters, the plastic degradation times, which usually take years, can be shortened to a few months [13,14]. This enables us to investigate degradation in a shortened time frame. The results of the discovered degradation processes could be important in the predictions on the long-term fate of plastic litter in the future.

Plastic degradation can be studied by characterizing the morphological or chemical changes induced by the environment. For morphological measurements, tools such as scanning electrode microscopy [15,16], atomic force microscopy [17] and X-ray computed tomography [18] are available. These tools can help us assessing the fragmentation sizes and rates that occur for certain environmental factors. To study molecular changes, non-destructive tools such as spectrophotometry [19], Fourier-transform infrared spectroscopy (FTIR) [20], nuclear magnetic resonance spectroscopy [16,21] and energy-dispersive X-ray spectroscopy [16] have already been employed. Such measurements can relate degradation processes with changes in the molecular structure that promote fragmentation or even the generation of toxic byproducts [12]. Overall, we see that findings on plastic degradation are typically acquired with tools that investigate the sample surface or the entire sample volume. A better understanding of degradation, however, requires a layer-by-layer analysis of the examined sample [22,23]. Such an analysis can be achieved with tools such as X-ray photoelectron spectroscopy, laser-ablation-inductively coupled plasma mass spectrometry (LA-ICP-MS) and mass spectrometry (GD-MS) [22,24]. Yet, these tools require specific sample shapes or long acquisition times or they have

* Corresponding author.
E-mail address: caroline.sommer@physik.uni-marburg.de (C. Sommer).

https://doi.org/10.1016/j.polymertesting.2022.107623
Received 23 February 2022; Received in revised form 6 April 2022; Accepted 2 May 2022
Available online 12 May 2022

poor resolutions [22]. Additionally, studies on degradation of plastic litter samples collected from the environment require an identification of the plastic type as a mandatory step [23]. Amongst those tools just mentioned only a few are used to investigate the plastic type of the sample.

A suitable candidate that can potentially identify the sample material and determine the chemical composition layer-by-layer simultaneously is laser-induced breakdown spectroscopy (LIBS). It is a type of atomic emission spectroscopy that gains information on the sample composition by generating a plasma on its surface. As the plasma decays, element-specific radiation is emitted and detected by a spectrometer. As a result, this technique is sensitive to almost all elements in the periodic table and hence, suitable to detect chemical changes and contamination. LIBS is commonly used for the investigation of metals [22,25–27] but it has already been demonstrated as a tool for depth profile studies [22,24,28]. Its potential for plastic identification has already been demonstrated for pristine plastic samples [29–31] and for microplastics [32]. Only few studies, however, have looked into its potential for plastic sample characterization [29–33]. Here, LIBS proved to be suitable to detect external elements in plastics such as encapsulated heavy metals [34,35] and remnants of corrosive gases [36]. To date, plastic degradation studies that use the layer-by-layer analysis capabilities of LIBS remain scarce. To the best of our knowledge, such studies have only been conducted by Brunnbauer et al. who investigated the degradation of artificially aged paint samples (a mixture of inorganic pigment and an organic polymeric binder) by evaluating the intensity of C2 and O with sample depth in an inert gas [36] and a spatially resolved classification of a multilayer system of 5 different synthetic polymers [37]. In the former, they show that the degradation of the paint samples become less pronounced with increasing sample depth. Although this proves that LIBS can be used to study degradation processes, it remains open if LIBS is sensitive enough to study different degradation stages of plastic litter which comprises of materials such as polystyrene (PS). Such an analysis can give an insight on the minimum time required for an environmental influence to induce chemical products inside the sample that could eventually escape.

Our study aims to close this gap by looking into the oxidation of different PS samples that were weathered with a standardized protocol [38]. PS is particularly interesting as weathering can generate one of the highest number of micro- and nanoparticles [39] which is essential for plastic litter mitigation studies. Additionally, PS is due to its carbon–carbon backbone susceptible to photo-oxidation, which is believed to be the most important abiotic degradation pathway in aerobic outdoor environments [12]. By evaluating the intensity of O with depth for PS at different weathering incubation times, we observe weathering-induced oxidation effects after around 400 h of artificial weathering. Thanks to the capability of LIBS to evaluate the sample composition with depth, we found potential additional insights on weathering-induced oxidation for PS that are not visible with surface detection methods. These results make LIBS stand out as a method that not only can identify plastic but also quantify the chemical composition inside the sample.

2. Materials and methods

2.1. Materials and accelerated weathering

This study used a series of commercially available, amorphous PS samples (INEOS Styrolution Group, Styrolution PS 158N) which contains 0 %, 0.5 % and 1 % concentrations of Irgafos 168, an antioxidant and processing stabilizer based on organophosphite. According to the manufacturer, this grade contained no additional additives besides 600 ppm of zinc stearate. For the accelerated weathering trials, type 1 A tensile bars were produced according to ISO 527-2 [40] via injection molding (Arburg GmbH, Arburg Allrounder 470H 1000-170).

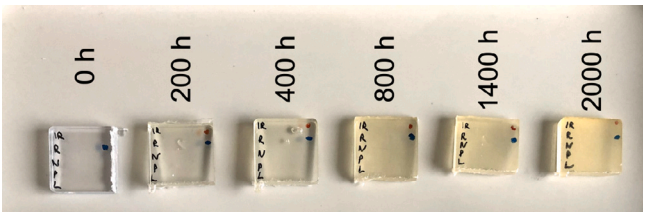

Fig. 1. A series of artificially weathered PS samples after different weathering times.

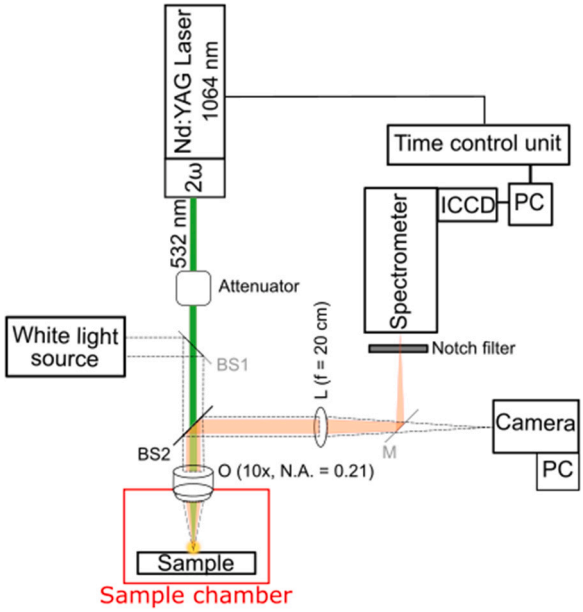

Fig. 2. Illustration of the built LIBS system used for measurements in different atmospheres.

The tensile bars were exposed to controlled accelerated weathering conditions following the standard ISO 4892-2:2011 [38]. For the weathering, an industrial test chamber (Q-LAB Corporation, Q-SUN XE-3) was used. To mimic the irradiation spectra of sunlight, the chamber was equipped with 3 xenon arc lamps and Daylight-Q filters. Following the standard, the irradiance intensity in the wavelength range 300–400 nm was set to 60 W/m^2. During the 102 min dry phase, the chamber temperature and relative humidity were set to 38 ° C and 55 %, respectively. During the stage of 18 min distilled water spraying, the temperature and the humidity were not controlled. For the analysis, samples after 200, 400, 800, 1400, and 2000 h of exposure were generated. A set of PS samples in different aging states is presented in Fig. 1.

2.2. Experimental setup

Fig. 2 shows the schematic of the experimental setup used to study the oxidation of plastics. A second harmonic Q-switched Nd:YAG laser (Quantel, Brilliant b model) with a repetition rate of 10 Hz, laser wavelength of 532 nm, pulse duration of 4 ns and maximum energy of 200 mJ was used as a radiation source. The laser pulse to generate the plasma on the sample's surface followed the pathway highlighted in green. First, it passed an attenuator, where its energy can be modified to adjust the ablation volume on the sample. After that, the pulse was focused vertically on the sample using a 10 x objective lens (O).

This arrangement created an approximately 80 μm diameter spot on the surface with an estimated power density of 9.95 × 10^{10} W/cm^2. A sample chamber was build around the sample holder to conduct measurements in an environment other than air. For this study, nitrogen

gas was used with a purity of 99.999 %. The relative humidity inside the chamber was between 0 %-10 %.

The optical path to acquire the sample's spectrum is highlighted in orange. A notch filter (Kaiser Optics, HSPF-532.0-1.0) was placed in front of the spectrometer to remove the incident laser pulse from the emitted light. The spectrum was recorded with a spectrometer (Newport corporation, MS257) that has a grating of 300 lines/mm and an entrance slit of 30 μm. It was equipped with a time-gated intensified charged-couple device (ICCD) camera (Andor, iStar DH720-18 U-03).

To investigate the ablation crater associated with LIBS measurements and to assure focal plane, a white light source and a camera were used. For this purpose, a detachable beamsplitter (BS1) and mirror (M) were integrated in the setup. The sample was then observed through the dashed optical pathway. To measure the depth of the crater, a profilometer was used (cyberTECHNOLOGIES, cyberSCAN CT 100). The lateral resolution was set to 5 μm.

For validation, FTIR measurements were conducted with a standalone FTIR microscope (Bruker, LUMOS II), operated with the spectroscopy software OPUS (version 8.5.29). The system was equipped with a single-element thermo-electrically cooled mercury-cadmium-telluride (TE-MCT) detector and a motorized germanium attenuated total reflection (ATR) crystal. The latter was applied to measure the samples with medium pressure.

2.3. Spectral acquisition

All LIBS spectra were acquired under the following conditions. The focal plane was set on the sample's surface, the pulse energy was adjusted to 20 mJ and the delay and gate width of the ICCD camera were set to 100 ns and 1000 ns, respectively. These settings were chosen in accordance to a report by Grègoire et al. which states that short delay widths produce signals with high signal-to-noise ratios for atomic signals while larger widths improve the ratio for molecular signals [30]. For this study, the delay width was optimized for the oxygen emission line. Since the C2 swan band system is also an important characterization parameter for plastics [32], the gate width was set to a higher value. Note that further optimizations of this parameter may be possible, but were not in the scope of this study.

The spectra were recorded in the spectral range 300 nm – 800 nm. This range was chosen based on the results of previous works [29,31,32]. Prior to a measurement, each sample was cleaned with 2-propanol. The measurements were performed in air or in nitrogen gas at atmospheric pressure where the gas flow was directed under the sample holder. The nitrogen gas prevented the air from interacting with the plasma and thus, interfering with the spectral signal.

To study weathering-induced oxidation on the sample's surface, a single-shot spectrum was acquired on 8 different sample locations. Measurements of the sample depth profile were acquired from 8 different spots that are separated by at least 200 μm. Each spot was hit 12 times by the laser pulse and the focal plane was adjusted after 3 consecutive shots. For the evaluation, the spectrum corresponding to a shot number, from now on referred to as layer, was averaged over all spots and their corresponding standard deviation was calculated. The depth of the layers was determined from the measurements by extracting the maximum depth in the crater area. Potential irregularities of the sample's surface, e.g. bumps or tilts, were also accounted for by fitting the surface with a polynomial function and subtracting it from the data.

For all spectra, the flatfield was recorded and the continuum background was subtracted to get rid of any possible error sources. This approach assured reliable and reproducible data and took any possible inhomogeneities into consideration that occur during the acquisitions.

For FTIR measurements, the sample and the background spectra were recorded with open aperture, 30 co-added scans, and a resolution of 4 cm^{-1} in the mid-infrared spectral range of 4000 cm^{-1}– 680 cm^{-1}. For each sample, one measurement was performed consisting of four replicated spots which were arranged in a square grid with distances of about 500 μm between each spot. The resulting spectra were averaged and processed for atmospheric influences in the spectral areas of carbon dioxide and water.

Table 1
List of relevant emission lines in the LIBS spectrum for PS [30–33,41].

Chemical species	Wavelength (nm)
C (I)	247.8
H	486.14, 656.29
O (I)	777.3
C2	470, 516.3, 553
CN	360, 388.3, 422
Ca (I)	422.69
Ca (II)	393.38, 396.83
Fe	557.8
K (I)	766.49, 769.89
Na (I)	589.15
N (I)	746.8

Table 2
List of absorption bands in ATR-FTIR spectrum formed by the oxidation processes in PS [36,42,43].

Functional group	Absorption band (cm^{-1})
ketone	1725
benzoic anhydride	1725, 1785
benzaldehyde	1704
benzophenone	1690
carboxylate	1553
benzoic acid dimer	1698
benzoic acid monomer	1732
dibenzoylmethane	1515, 1605
dimeric acetic and formic acid	1710
hydroxyl region	3000–3600
C-O region	1100–1200
C=O region	1732

2.4. Spectral line identification

The characteristic peaks for the spectral fingerprint of plastics in LIBS are the atomic and ionic emission lines of the hydrogen Balmer series, the carbon line and the oxygen line, as well as the diatomic molecular bands of the C2 swan band and the CN violet band [30–33]. In addition, peaks coming from additives within the sample or from contamination on the sample's surface such as calcium, iron, sodium, nitrogen and potassium are also inevitable. For the characterization of weathering-induced oxidation of PS, this work will only focus on the oxygen emission line at 777.3 nm. Note that the carbon line is not detected with this setup as it lies in the deep UV range. All relevant peaks are summarized in Table 1.

For the evaluation with FTIR, the main and secondary absorption bands formed by the oxidation processes in PS are used as reported by numerous studies [36,42,43] and summarized in Table 2. The sum of the intensities of all these absorption bands was calculated and used as input. Here, we follow the same approach as Brunnbauer et al. [36].

3. Results and discussion

3.1. Influence of atmospheres on laser-induced plasma

When conducting LIBS measurements in an environment other than vacuum, additional contributions from the environment to the emission spectrum are possible. These contributions must be considered first before conclusions can be drawn from the spectral data. Since this study focuses on the presence of oxygen in the sample, conducting measurements in ambient air may not be wise because of possible contributions from the surrounding oxygen. To further look into this, the spectrum of weathered PS measured in ambient air is evaluated first. Fig. 3a shows the spectra of two PS samples after 0 h (red) and 2000 h (blue) of weathering measured in air. The superposition reveals additional peaks in the spectrum for 2000 h weathered PS compared to untreated PS. The additional peaks not belonging to the

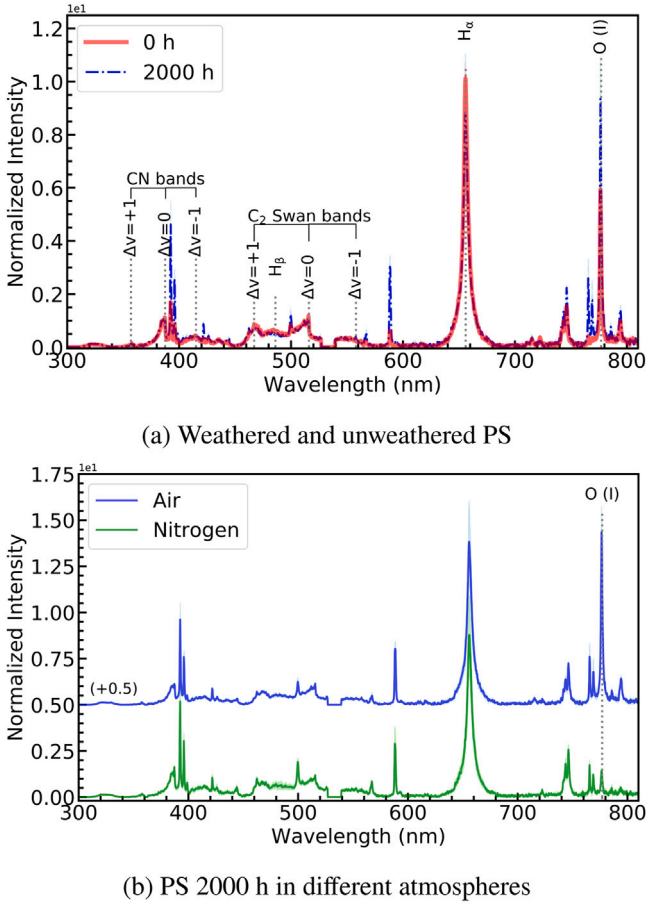

Fig. 3. LIBS spectra from PS 0 h and PS 2000 h in different atmospheres. (a) shows the samples PS 0 h and PS 2000 h measured in air. Apart from the peaks coming from additives, the aging seems to only have influenced the oxygen peak from the characteristic plastic peaks (CN, C2, H, O). (b) shows sample PS 2000 h measured in air and nitrogen atmosphere. It shows that the oxygen peak is highly influenced by air. The spectra are the average over 3 measurements (average is depicted as line, standard deviation as light background). For better comparability, the spectra are normalized to C2 ($\Delta v = 0$). In (b) the spectra are plotted with an offset.

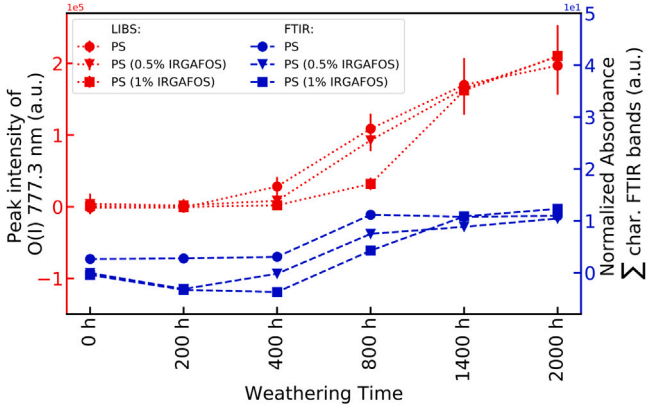

Fig. 4. Course of oxidation at different weathering times. The plot shows the detected oxidation level for LIBS (oxygen intensity at 777.3 nm is shown on the left axis) and FTIR (sum of characteristic peaks representing the spectral fingerprint of chemical processes generated by oxidation is shown on the right axis). Each LIBS data point is the average over 8 measurements (average is depicted as a symbol, standard deviation as line). Each FTIR data point is the average over 4 measurements and normalized to CO_2 and hydrogen bands.

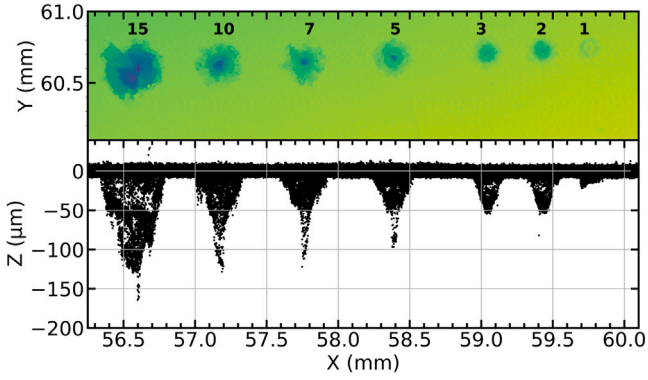

Fig. 5. Surface measurement from 2000 h weathered PS (1% Irgafos) The plot shows the crater depth from 1 to 15 shots. In addition it shows the embrittlement of the sample's surface. In order to determine the crater depth precisely, the unevenness of the surface was fitted and straightened using a polynomial function.

polymer matrix of PS are listed in the second half of Table 1. These occurrences originate from contaminations on the porous surface which develop during the weathering treatment. A comparison of the oxygen peak at 777.3 nm for both samples shows an increase in intensity for 2000 h weathered PS which implies a higher oxygen content due to weathering. Yet, the measurements raise the question of why the unweathered sample (red) shows an oxygen peak at all when there is no oxygen in its chemical structure. Fig. 3b helps to shed light on this issue. The plot shows the 2000 h weathered sample measured in air and in nitrogen. Depending on the atmosphere, the oxygen peak is more than 6 times more intense. This demonstrates the significant influence of air on the oxygen peak. Therefore, it is advised not to use air as surrounding atmosphere for weathering-induced oxidation. Nitrogen, however, appears to be a more suitable atmosphere for oxidation measurements and is additionally a more sustainable alternative as opposed to inert gases used elsewhere [36]. These findings agree with other previous reports that the surrounding sample environment can bias the observations [44,45]. Therefore, this work will not quantify the influences of different gases on the spectra.

Note that although contaminations are present in weathered samples, the spectral fingerprint for PS can still be identified in the spectrum (see Fig. 3a and Table 1). This underlines the suitability of LIBS as an identification method for plastic materials.

3.2. Oxygen intensity with regard to weathering time

As mentioned earlier, weathering-induced oxidation is studied with LIBS by evaluating the oxygen intensity in different samples. This raises the question if the results are comparable to already established methods. In the following, LIBS measurements on the sample surface for different weathering times are compared to those measured with FTIR. The spectral data acquired with the latter can be found in the supplements.

Fig. 4 shows surface measurements with LIBS (dotted, red) and FTIR (dashed, blue) for PS, PS (0.5 % Irgafos) and PS (1 % Irgafos) at different weathering times. In the LIBS procedure, the oxygen intensity increases after 400 h of weathering. Before that, the oxidation is hardly observable. At 800 h, the measurements for PS (1 % Irgafos) stand out since the increase of the oxygen peak is clearly lower than in the other samples. Reason for this may be due to the higher concentration of Irgafos. However, after 800 h the oxygen peak increases rapidly and reaches a value comparable to the one of the other samples. As Irgafos slows down the weathering-induced oxidation of PS by decomposing the generated hydroperoxide or by limiting the formation of peroxide radicals by trapping the oxygen present into the bulk of the polymer [46], the oxidation can only be delayed as long as the additive is not used up. After 800 h, this seems to have occurred and the oxygen

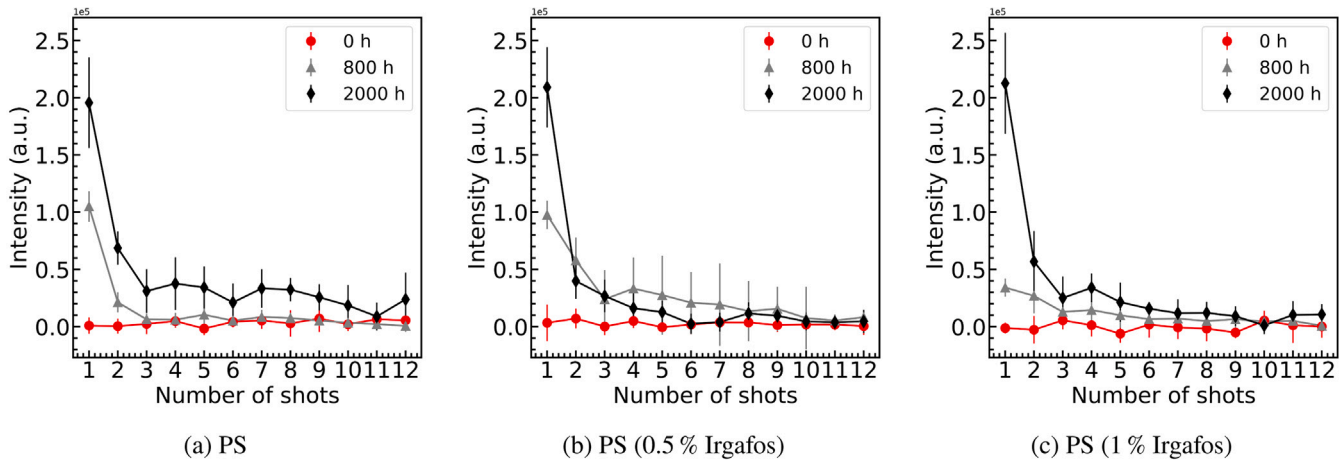

Fig. 6. Oxygen intensity with depth for different samples up to 2000 h of weathering time. The plot shows the decrease of the oxygen intensity with increasing number of shots inside the sample. 12 shots correspond to a depth of approximately (111.39 ± 9.97) μm.

content increases steeply. Note that the contribution of Irgafos to the oxygen intensity in the LIBS signal is negligible due to the small amount of Irgafos compared to the reaction coming from photo-oxidation. It should also be mentioned that the analysis of the oxidized form of Irgafos is not the focus of this work and we refer to [46] for more details on this topic.

In the FTIR measurements the absorbance increases after 400 h of weathering and starts to saturate for weathering times larger than 1400 h. Potential reasons for this saturation have already been discussed in [16]. It is explained that the oligomers derived from polymer chains become shorter and their polarities become high enough so that they dissolve in water and are rinsed out during the cleaning protocol [16]. However, in the LIBS measurements this saturation has not been observed. This may be due to the fact that LIBS measures at larger depths than FTIR. One LIBS shot has an ablation depth of approximately (23.53 ± 4.91) μm, compared to a maximum penetration depth of 6 μm for ATR-FTIR. Accordingly, in LIBS the oxygen content is averaged over a larger volume. Since some of the ketone groups in the surface are rinsed out, saturation occurs in FTIR measurements [16], while LIBS includes oxidation that occur in deeper layers which do not rinse out easily. This could explain the difference in the data from 800 h onwards in Fig. 4. It can be said that the trend of the course of oxidation received from the LIBS measurements are in good agreement with the FTIR results.

The comparison shows that the use of ATR-FTIR as a sole characterization method raises questions that need further explanation, such as the saturation observed earlier. Here, LIBS can provide additional details because of its larger penetration depth and thus, both techniques may complement each other. Furthermore, for weathering-induced oxidation the evaluation in LIBS is more convenient than in FTIR, since the former only needs to analyze one peak while the latter has to identify and include all relevant absorption bands.

3.3. Depth profile analysis

In the following, depth profiles of PS, PS (0.5 % Irgafos) and PS (1 % Irgafos) at 3 different weathering times (0 h, 800 h, and 2000 h) are generated using LIBS.

In order to evaluate the depth of the crater after each laser shot, referred to as layer, a pattern with 1, 2, 3, 5, 7, 10 and 15 shots was generated. This profile was made under the same conditions as the depth profile measurements described in chapter 2.3. Fig. 5 shows an example of a profilometer measurement for the craters corresponding to a different number of laser shots. The plot reveals that the ablation depth increases with the number of shots. With this measuring procedure a total depth of (111.39 ± 9.97) μm for 12 layers were achieved. The thick strip of data points around the height Z = 0 μm illustrates the increased surface roughness due to weathering.

Fig. 6 shows the propagation of the oxidation into the samples PS, PS (0.5 % Irgafos) and PS (1 % Irgafos). The oxygen intensity for the unweathered samples (red, ●) remains unchanged regardless of whether measurements are taken on the surface or inside the sample. The depth profiles indicate that the oxidation for a weathering time of 800 h for all samples (gray, ▲) extends into the second layer with a depth of approximately (51.23 ± 11.21) μm. For samples that were weathered for 2000 h (black, ♦), the oxidation penetrates into the third layer with a depth of approximately (57.98 ± 6.36) μm. This proves that the oxygen content as well as its penetration depth varies with weathering time. The influence of the additive concentration can be observed by evaluating the oxygen intensity in the second layer. In PS the oxygen intensity for 800 h and 2000 h are clearly distinguishable (see Fig. 6(a)). However, the oxygen intensity for PS (0.5 % Irgafos) and PS (1 % Irgafos) for a weathering time of 800 h and 2000 h are within the scope of their error bars equal in the second layer. Even though the penetration depth is the same for all samples, the trend of the oxygen peak in PS with additives appears to be flatter than in PS with no additives for a weathering time of 800 h. At 2000 h, however, no influence of the oxidation process is visible which could be due to the fact that the additive has already been used up (see Fig. 6). This may imply that oxidation penetrates less intense into the samples with higher concentration. Such a behavior is in agreement with the findings of Gijsman et al. who showed that the oxidation-depth profile of PA with an antioxidant is much flatter than for PA without the antioxidant [47]. Overall, the results illustrate that LIBS is sufficiently sensitive to perform a layer-by-layer analysis to identify changes in the sample's chemical structure due to weathering-induced oxidation.

4. Conclusion

The low biodegradability of plastic does not only lead to an accumulation of plastic litter in the environment but also to its exposure to various weathering and aging processes. In this study, we focus on weathering-induced oxidation for polystyrene (PS) samples. The aim was to systematically study this effect on the sample's surface and its depth profile at different weathering times (0 h, 200 h, 400 h, 800 h, 1400 h, 2000 h) using LIBS as an analytical tool.

During the course of this study, 3 sets of samples with different additive concentrations were analyzed in nitrogen gas. It was shown that ambient gas can have strong effects on LIBS measurements. Therefore, an atmosphere that does not contain oxygen is recommended for measuring the degree of weathering-induced oxidation. In this context,

nitrogen has proven to be a cost-efficient alternative compared to inert gases.

The PS samples used in this study showed increased oxygen peaks with weathering time starting from 400 h in the LIBS spectra. Similar results were also obtained with FTIR. There, increased absorption bands formed by oxidation processes were detected from 400 h onwards compared to unweathered samples. This confirms that LIBS is sensitive enough to measure oxidation on the sample's surface. Due to laser ablation, LIBS is also capable of depth profile analysis and therefore, the penetration depth of the oxidation could be evaluated. In the weathered samples increased oxygen peaks were detected up to (57.98 ± 6.36) μm. The addition of Irgafos appears to hinder the penetration of oxygen with weathering time until the additive has been used up. Overall, these results illustrate that LIBS could provide valuable insights on the degradation of plastics in the environment that are not visible with common analytical tools.

To date, most studies on plastic pollution use FTIR, which has established itself as a non-destructive tool for (micro-) plastic identification [48–51]. It derives details on the chemical structure of the sample by looking at interactions between infrared light and functional groups in a molecule. To conduct a layer-by-layer analysis similar to our study but with FTIR, the sample must be prepared, e.g. with a microtome, to expose the sample's cross-section which can be more difficult as the sample size decreases, e.g. for microplastics. In comparison, LIBS primarily evaluates the emission signals from atoms that belong to the target material. While this technique is minimal destructive due to laser ablation, a layer-by-layer analysis does not require any sample preparation. Both can, therefore, be considered as complementary spectroscopic techniques that determine and validate the properties of the sample. This motivates further research on LIBS' application on degraded plastic litter samples from the environment as well as the comparability of the results measured with LIBS and FTIR. Additionally, a larger sample set should be evaluated in order to obtain statistically meaningful results.

In conclusion, considering LIBS' ability to combine plastics identification, trace element detection and, as shown in the present study, the detection of weathering-induced-oxidation, this technique has the potential to establish itself as a promising identification and analysis tool for plastic litter.

CRediT authorship contribution statement

Caroline Sommer: Conceptualization, Methodology, Investigation, Software, Formal analysis, Visualization, Validation, Writing – original draft, Writing – review & editing. **Johnny Nguyen:** Conceptualization, Methodology, Supervision, Software, Formal analysis, Investigation, Writing – original draft, Writing – review & editing. **Teresa Menzel:** Resources, Writing – review & editing. **Julia A. Prume:** Investigation, Validation, Writing – review & editing. **Holger Ruckdäschel:** Project administration, Writing – review & editing. **Martin Koch:** Project administration, Writing – review & editing.

Declaration of competing interest

The authors declare that they have no known competing financial interests or personal relationships that could have appeared to influence the work reported in this paper.

Data availability

The data is available from the corresponding author.

Acknowledgments

We thank Dr. Frank Noll and Dr. Hee-Cheol Kim for providing their expertise for the profilometer measurements and Felix Gorka for support and helping interpreting the FTIR data.

Funding

Part of this project was funded by the Deutsche Forschungsgemeinschaft (DFG, German Research Foundation) - Project Number 391977956 - SFB 1357, subproject C01. Open Access funding was provided by the Open Acess Publication Fund of Philipps-Universität Marburg with support of the Deutsche Forschungsgemeinschaft (DFG, German Research Foundation).

Appendix A. Supplementary data

Supplementary material related to this article can be found online at https://doi.org/10.1016/j.polymertesting.2022.107623.

References

[1] H. Ritchie, M. Roser, Plastic pollution, Our World in Data (2018).
[2] C.M. Rochman, M.A. Browne, A.J. Underwood, J.A. van Franeker, R.C. Thompson, L.A. Amaral-Zettler, The ecological impacts of marine debris: unraveling the demonstrated evidence from what is perceived, Ecology 97 (2) (2016) 302–312.
[3] A.D. Vethaak, H.A. Leslie, Plastic debris is a human health issue, Environ. Sci. Technol. 50 (13) (2016) 6825–6826.
[4] C.M. Rochman, M.A. Browne, B.S. Halpern, B.T. Hentschel, E. Hoh, H.K. Karapanagioti, L.M. Rios-Mendoza, H. Takada, S. Teh, R.C. Thompson, Classify plastic waste as hazardous, Nature 494 (7436) (2013) 169–171.
[5] B. Toussaint, B. Raffael, A. Angers-Loustau, D. Gilliland, V. Kestens, M. Petrillo, I.M. Rio-Echevarria, G. Van den Eede, Review of micro- and nanoplastic contamination in the food chain, Food Addit. Contamin.: A 36 (5) (2019) 639–673.
[6] L.G.A. Barboza, C. Lopes, P. Oliveira, F. Bessa, V. Otero, B. Henriques, J. Raimundo, M. Caetano, C. Vale, L. Guilhermino, Microplastics in wild fish from North East Atlantic Ocean and its potential for causing neurotoxic effects, lipid oxidative damage, and human health risks associated with ingestion exposure, Sci. Total Environ. 717 (2020) 134625.
[7] M. Haave, A. Gomiero, J. Schönheit, H. Nilsen, A.B. Olsen, Documentation of microplastics in tissues of Wild Coastal animals, Front. Environ. Sci. 9 (2021).
[8] A.J. Jamieson, L.S.R. Brooks, W.D.K. Reid, S.B. Piertney, B.E. Narayanaswamy, T.D. Linley, Microplastics and synthetic particles ingested by deep-sea amphipods in six of the deepest marine ecosystems on Earth, R. Soc. Open Sci. 6 (2) (2019) 180667.
[9] A.A. Koelmans, N.H. Mohamed Nor, E. Hermsen, M. Kooi, S.M. Mintenig, J. De France, Microplastics in freshwaters and drinking water: Critical review and assessment of data quality, Water Res. 155 (2019) 410–422.
[10] A. Ragusa, A. Svelato, C. Santacroce, P. Catalano, V. Notarstefano, O. Carnevali, F. Papa, M.C.A. Rongioletti, F. Baiocco, S. Draghi, E. D'Amore, D. Rinaldo, M. Matta, E. Giorgini, Plasticenta: First evidence of microplastics in human placenta, Environ. Int. 146 (2021) 106274.
[11] A.L. Andrady, Microplastics in the marine environment, Mar. Pollut. Bull. 62 (8) (2011) 1596–1605.
[12] B. Gewert, M.M. Plassmann, M. MacLeod, Pathways for degradation of plastic polymers floating in the marine environment, Environ. Sci.: Processes Impacts 17 (9) (2015) 1513–1521.
[13] A.S. Maxwell, W.R. Broughton, G.D. Dean, G.D. Sims, Review of Accelerated Ageing Methods and Lifetime Prediction Techniques for Polymeric Materials, NPL Report, National Physical Laboratory, 2005.
[14] P. Liu, Y. Shi, X. Wu, H. Wang, H. Huang, X. Guo, S. Gao, Review of the artificially-accelerated aging technology and ecological risk of microplastics, Sci. Total Environ. 768 (2021) 144969.
[15] B. Suresh, S. Maruthamuthu, M. Kannan, A. Chandramohan, Mechanical and surface properties of low-density polyethylene film modified by photo-oxidation, Polymer J. 43 (4) (2011) 398–406.
[16] N. Meides, T. Menzel, B. Poetzschner, M.G.J. Löder, U. Mansfeld, P. Strohriegl, V. Altstaedt, J. Senker, Reconstructing the environmental degradation of polystyrene by accelerated weathering, Environ. Sci. Technol. (2021).
[17] N. Ojha, N. Pradhan, S. Singh, A. Barla, A. Shrivastava, P. Khatua, V. Rai, S. Bose, Evaluation of HDPE and LDPE degradation by fungus, implemented by statistical optimization, Sci. Rep. 7 (1) (2017) 39515.
[18] S. Garcea, Y. Wang, P. Withers, X-ray Computed tomography of polymer composites, Compos. Sci. Technol. 156 (2018) 305–319.
[19] C.P. Ward, C.J. Armstrong, A.N. Walsh, J.H. Jackson, C.M. Reddy, Sunlight converts polystyrene to carbon dioxide and dissolved organic carbon, Environ. Sci. Technol. Lett. 6 (11) (2019) 669–674.

[20] M. Celina, D. Ottesen, K. Gillen, R. Clough, FTIR emission spectroscopy applied to polymer degradation, Polym. Degrad. Stab. 58 (1–2) (1997) 15–31.
[21] N. Peez, M.-C. Janiska, W. Imhof, The first application of quantitative 1H NMR spectroscopy as a simple and fast method of identification and quantification of microplastic particles (PE, PET, and PS), Anal. Bioanal. Chem. 411 (4) (2019) 823–833.
[22] T. Canel, P. Demir, E. Kacar, B.G. Oztoprak, E. Akman, M. Gunes, A. Demir, Optimization of parameters for depth resolution of galvanized steel by LIBS technique, Opt. Laser Technol. 54 (2013) 257–264.
[23] N.P. Ivleva, Chemical analysis of microplastics and nanoplastics: Challenges, advanced methods, and perspectives, Chem. Rev. 121 (19) (2021) 11886–11936.
[24] M.P. Mateo, G. Nicolas, V. Pinon, A. Yanez, Improvements in depth-profiling of thick samples by laser-induced breakdown spectroscopy using linear correlation, Surf. Interf. Anal. Int. J. Devot. Dev. Appl. Tech. Anal. Surf. Interfaces Thin Films 38 (5) (2006) 941–948.
[25] H. Balzer, M. Hoehne, R. Noll, V. Sturm, New approach to online monitoring of the Al depth profile of the hot-dip galvanised sheet steel using LIBS, Anal. Bioanal. Chem. 385 (2) (2006) 225–233.
[26] S. Couris, A. Hatziapostolou, D. Anglos, A. Mavromanolakis, C. Fotakis, Laser-induced breakdown spectroscopy (LIBS) applications in environmental issues, in: ALT'96 International Symposium on Laser Methods for Biomedical Applications, vol. 2965, International Society for Optics and Photonics, 1996, pp. 83–87.
[27] V. Dwivedi, A. Marín-Roldán, J. Karhunen, P. Paris, I. Jõgi, C. Porosnicu, C. Lungu, H. van der Meiden, A. Hakola, P. Veis, CF-LIBS quantification and depth profile analysis of Be coating mixed layers, Nucl. Mater. Energy 27 (2021) 100990.
[28] G. Galbács, A critical review of recent progress in analytical laser-induced breakdown spectroscopy, Anal. Bioanal. Chem. 407 (25) (2015) 7537–7562.
[29] R. Sattmann, I. Monch, H. Krause, R. Noll, S. Couris, A. Hatziapostolou, A. Mavromanolakis, C. Fotakis, E. Larrauri, R. Miguel, Laser-induced breakdown spectroscopy for polymer identification, Appl. Spectrosc. 52 (3) (1998) 456–461.
[30] S. Grégoire, M. Boudinet, F. Pelascini, F. Surma, V. Detalle, Y. Holl, Laser-induced breakdown spectroscopy for polymer identification, Anal. Bioanal. Chem. 400 (10) (2011) 3331–3340.
[31] D. Stefas, N. Gyftokostas, E. Bellou, S. Couris, Laser-induced breakdown spectroscopy assisted by machine learning for plastics/polymers identification, Atoms 7 (3) (2019) 79.
[32] C. Sommer, L. Schneider, J. Nguyen, J. Prume, K. Lautze, M. Koch, Identifying microplastic litter with laser induced breakdown spectroscopy: A first approach, Mar. Pollut. Bull. 171 (2021) 112789.
[33] M.V. Dastjerdi, S.J. Mousavi, M. Soltanolkotabi, A.N. Zadeh, Identification and sorting of PVC polymer in recycling process by laser-induced breakdown spectroscopy (LIBS) combined with support vector machine (SVM) model, Iran. J. Sci. Technol. Trans. A Sci. 42 (2) (2018) 959–965.
[34] X. Chen, S. Ali, L. Yuan, F. Guo, G. Huang, W. Shi, X. Chen, Characterization and source analysis of heavy metals contamination in microplastics by Laser-Induced Breakdown Spectroscopy, Chemosphere 287 (2022) 132172.
[35] D. Chen, T. Wang, Y. Ma, G. Wang, Q. Kong, P. Zhang, R. Li, Rapid characterization of heavy metals in single microplastics by laser induced breakdown spectroscopy, Sci. Total Environ. 743 (2020) 140850.
[36] L. Brunnbauer, M. Mayr, S. Larisegger, M. Nelhiebel, L. Pagnin, R. Wiesinger, M. Schreiner, A. Limbeck, Combined LA-ICP-MS/LIBS: powerful analytical tools for the investigation of polymer alteration after treatment under corrosive conditions, Sci. Rep. 10 (1) (2020) 12513.
[37] L. Brunnbauer, S. Larisegger, H. Lohninger, M. Nelhiebel, A. Limbeck, Spatially resolved polymer classification using laser induced breakdown spectroscopy (LIBS) and multivariate statistics, Talanta 209 (2020) 120572.
[38] ISO 4892-2:2011, Plastics — Methods of exposure to laboratory light sources — Part 2: Xenon-arc lamps, International Organization for Standardization, 2011.
[39] S. Lambert, M. Wagner, Characterisation of nanoplastics during the degradation of polystyrene, Chemosphere 145 (2016) 265–268.
[40] ISO 527-2:2012, Plastics — Determination of Tensile Properties — Part 2: Test Conditions for Moulding and Extrusion Plastics, Technical Report, International Organization for Standardization, Geneva, CH, 2012, p. 11.
[41] A. Kramida, Y. Ralchenko, J. Reader, N.A. Team, NIST Atomic Spectra Database (version 5.9), National Institute of Standards and Technology, Gaithersburg, 2021, http://dx.doi.org/10.18434/T4W30F.
[42] C. Sandt, J. Waeytens, A. Deniset-Besseau, C. Nielsen-Leroux, A. Réjasse, Use and misuse of FTIR spectroscopy for studying the bio-oxidation of plastics, Spectrochim. Acta A 258 (2021) 119841.
[43] B. Mailhot, J.L. Gardette, Polystyrene photooxidation. 1. Identification of the IR-absorbing photoproducts formed at short and long wavelengths, Macromolecules 25 (16) (1992) 4119–4126.
[44] M. Dong, X. Mao, J.J. Gonzalez, J. Lu, R.E. Russo, Time-resolved LIBS of atomic and molecular carbon from coal in air, argon and helium, J. Anal. At. Spectrom. 27 (12) (2012) 2066.
[45] S.J. Mousavi, M.H. Farsani, S.M.R. Darbani, A. Mousaviazar, M. Soltanolkotabi, A.E. Majd, CN and C 2 vibrational spectra analysis in molecular LIBS of organic materials, Appl. Phys. B 122 (5) (2016) 106.
[46] K. Fouyer, O. Lavastre, D. Rondeau, Direct monitoring of the role played by a stabilizer in a solid sample of polymer using direct analysis in real time mass spectrometry: the case of irgafos 168 in polyethylene, Anal. Chem. 84 (20) (2012) 8642–8649.
[47] P. Gijsman, W. Dong, A. Quintana, M. Celina, Influence of temperature and stabilization on oxygen diffusion limited oxidation profiles of polyamide 6, Polym. Degrad. Stab. 130 (2016) 83–96.
[48] A. Bellasi, G. Binda, A. Pozzi, S. Galafassi, P. Volta, R. Bettinetti, Microplastic contamination in freshwater environments: A review, focusing on interactions with sediments and benthic organisms, Environments 7 (4) (2020) 30.
[49] A. Käppler, D. Fischer, S. Oberbeckmann, G. Schernewski, M. Labrenz, K.-J. Eichhorn, B. Voit, Analysis of environmental microplastics by vibrational microspectroscopy: FTIR, Raman or both? Anal. Bioanal. Chem. 408 (29) (2016) 8377–8391.
[50] E.C. Minor, R. Lin, A. Burrows, E.M. Cooney, S. Grosshuesch, B. Lafrancois, An analysis of microlitter and microplastics from lake superior beach sand and surface-water, Sci. Total Environ. 744 (2020) 140824.
[51] S. Primpke, C. Lorenz, R. Rascher-Friesenhausen, G. Gerdts, An automated approach for microplastics analysis using focal plane array (FPA) FTIR microscopy and image analysis, Anal. Methods 9 (9) (2017) 1499–1511.